Analytical investigation of adhesion in metals/ceramic systems via elastic parameters

Z. HADEF, A. DOGHMANE*, Z. HADJOUB
Laboratoire des Semi-Conducteurs, Département de Physique, Faculté des Sciences, Université Badji-Mokhtar, BP 12, Annaba, DZ-23000, Algérie

Metal/ceramics substrates are of great importance in many technological applications and fundamental understanding of physical behavior of the adhesion between two different materials. In this context, we investigate the dependence of adhesion energy, W_{ad}, on elastic parameters of these systems. To do so, we considered several metals (Au, Cu, Sn, Ga and Ag) on a great number of ceramic substrates (AlN, Al_2O_3, BN, CoO, Er_2O_3, Ho_2O_3, LaB_6, Lu_2O_3, MgO, NiO, SiC, SiO_2, Si_3N_4, TiC, TiO, TiO_2, Ti_2O_3, Y_2O_3, Yb_2O_3, ZnO and Zr_2O_3). Different approaches are used. Semi-empirical relations are deduced for all systems. It is shown that, in all cases, the adhesion energy increases linearly with Rayleigh velocities, V_R; it takes the form: $W_{ad.} = 0.07\ V_R + C$. However, the characteristic term C strongly depends on the system combination as well as on the energy gap of the ceramics: it is higher for small gap materials due to the ease of electron transfer through the metal/ceramic interface and vice-versa. The importance of this relation lies in its universality and applicability to all investigated combinations. Moreover, it could be extended, through familiar relations, to other elastic parameters.

(Received March 12, 2018; accepted October 10, 2018)

Keywords: Adhesion, Energy gap, Ceramics, Metals, Elastic parameters

1. Introduction

Metalized ceramics play an important role in several modern technological applications such as electrical devices, metal films on ceramic substrates, metal-ceramic bonding, ceramic-metal matrix composites, etc. However, the coating of ceramic surfaces can affect most of the properties of the interface. Therefore, the investigation of interfacial phenomena between metals and ceramic substrates is of great importance not only in technological applications but also in fundamental understanding of physical behavior of the adhesion between two different materials as far as their electrical structures and physiochemical properties are concerned. In fact, at the interface of a metal/ceramic system, adhesion occurs when the atoms or molecules of the two contacting surfaces approach each other so closely that attractive forces between approaching atoms (or molecules) bond them together. The strength of the bond depends on the size of the atoms, the distance between them, and the presence or absence of contaminant matter on the surface [1]. Hence, the strength or wea1kness of bonds is the key factor to determine the interface stability: good adhesion, welded adhesion, perfect bonding, weak bonding smooth interface, etc. The metal/ceramic contact is characterized by the adhesion energy, W_{ad}, which is the work per unit area of the interface needed to separate reversibly a metal/ceramic interface [2].

At the interface zone, the surface acoustic wave, SAW propagation which depends on elastic properties of solid substrates are greatly affected: the response would be different depending on the weakness or strength of bonds due to impedance mismatching [3]. Hence, in this context, we investigate the dependences of adhesion energy on elastic parameters, in particular SAW velocities, for many metal/ceramic systems.

2. Calculation procedure and conditions

2.1. Methodology

Elastic properties can be determined non-destructively via ultrasonic investigations; the techniques consist of determining surface acoustic wave, SAW, velocities (longitudinal, V_L, transverse, V_T and Rayleigh, V_R) from which elastic constants such Young's modulus, E, is deduced according to the well established conventional relation and vice versa, i.e.:

$$E = \rho V_T^2 \left(\frac{3\rho V_L^2 - 4\rho V_T^2}{\rho V_L^2 - \rho V_T^2} \right) \quad (1)$$

where ρ is the materials density.

In this work, two approaches are adopted: (i) one parameter approach [4] and (ii) the scanning acoustic microscope, SAM, approach [5, 6]. The former consists of using the simplified familiar relations of elastic constants (given as a function of V_L and V_T) into simple relations. Hence, E is expressed in terms of the velocity of just one single mode (V_L, V_T, V_R), as we recently reported [4].

$$E = 2.99\rho V_R^2 \quad = 0.557\rho V_L^2 \quad = 2.586\rho V_T^2 \quad (2)$$

The second SAM approach consists of theoretical determination of these velocities from the so-called acoustic materials signatures, also known as V(z) response [5, 6]. Such a signature describes the output response, V, as a function of the defocusing distance, z.

Experimentally, the most used instrument for this a purpose is the scanning acoustic microscope [7]. Such curves, can also be calculated via the angular spectrum model proposed by Sheppard and Wilson [8] who derived the following expression:

$$V(z)=\int P^2(\theta)R(\theta)\exp(2jk_o z\cos\theta)\sin\theta\cos\theta d\theta \quad (3)$$

Here $P^2(\theta)$ is the pupil function, θ is the half-opening angle of the lens, z is the defocusing distance and $k_o = 2\pi/\lambda$ is the wave number in the coupling liquid, $j = \sqrt{-1}$ and $R(\theta)$ is the reflection coefficient that is given by:

$$R(\theta) = \left(\frac{Z_L \cos^2 2\theta_T + Z_T \sin^2 2\theta_T - \rho_{ilq} V_{liq} / \cos\theta}{Z_L \cos^2 2\theta_T + Z_T \sin^2 2\theta_T + \rho_{ilq} V_{liq} / \cos\theta} \right) \quad (4)$$

where ρ_{liq}, V_{liq}, Z_L, Z_T and θ_T are the liquid density, liquid velocity, longitudinal impedance, transverse impedance and critical angle at which transverse modes are excited in the material, respectively.

The steps of the SAM approach, consist of determining SAW velocities of different modes, calculating acoustic materials signatures and deducing SAW velocities via fast Fourier transform, FFT, treatment of periodic V(z) signatures. The details of these steps can be found elsewhere [9-11].

2.2. Materials and simulation conditions

In this investigation, we consider several metals (Au, Cu, Sn, Ga and Ag) on a great number of ceramic substrates (AlN, Al_2O_3, BN, CoO, Er_2O_3, Ho_2O_3, LaB_6, Lu_2O_3, MgO, NiO, SiC, SiO_2, Si_3N_4, TiC, TiO, TiO_2, Ti_2O_3, Y_2O_3, Yb_2O_3, ZnO and Zr_2O_3). The characteristics of all materials: energy gap, E_g [12] density, ρ, and Young's modulus, E, [7] are listed in Table 1.

The simulation conditions are those usually used experimentally in the case of a reflexion scanning acoustic microscope, SAM [7, 9-11]: a half opening angle of the lens of 50°, an operating frequency, f = 140 MHz and water as a coupling liquid whose wave velocity, V_{liq}= 1500 m/s and density, ρ = 1000 kg/m^3.

3. Results and discussions

3.1. Acoustic signatures and treatment

In the one parameter approach, we used simplified relations (2) and some published data [7, 12] of ρ and E, to determine SAW velocities; the results are grouped in Table 1. The, obtained data of V_L and V_T are then used in the SAM approach, i.e., they are injected in relations 3 and 4 to deduce the V(z) curves of all substrate materials.

Typical V(z) results are illustrated in Fig. 1a for two bulk substrates BN (- - - -) and Al_2O_3 (——); it should be noted that similar curves were obtained for all other ceramic substrates. It is clear that both curves exhibit oscillatory behavior due to constructive and destructive interferences between axial beams and the reflected leaky waves, in the reflection SAM configuration.

Table 1. Characteristics of investigated materials: energy gap, E_g, density, ρ, and Young's modulus, E, as well as the determined SAW velocities (longitudinal, V_L, transverse, V_T and Rayleigh V_R)

Ceram. Subst.	ρ (kg/m^3) [7]	E (GPa) [7]	E_g (eV) [12]	Calculated SAW velocities			
				V_L (m/s)	V_T (m/s)	$V_R]_1$ (m/s)	$V_R]_{sam}$ (m/s)
AlN	3260	318	5.6	11367	6169	5712	5616
Al_2O_3	3980	330	7.1	11437	6207	5747	5650
BN	3487	34	8.1	3594	1950	1806	1834
CoO	9423	281	0.5	5725	3107	2877	2871
Er_2O_3	8651	179	3.2	5236	2841	2631	2633
Ho_2O_3	8414	175	3.9	5248	2848	2637	2639
Lu_2O_3	9423	204	4.0	5355	2906	2691	2691
MgO	3580	310	7.3	10710	5813	5382	5297
NiO	6670	420	2.5	12579	6827	6321	6205
SiC	3210	393	3.3	13626	7395	6847	6714
SiO_2	2600	75	7.9	7383	4007	3710	3678
TiC	4940	400	0.3	10861	5895	5458	5370
TiO	4950	387	0.0	7964	4322	4002	3960
TiO_2	4230	315	3.1	9932	5390	4991	4917
Ti_2O_3	4468	118	0.1	8891	4825	4468	4411
Y_2O_3	5030	176	5.5	6808	3695	3421	3398
Yb_2O_3	9293	229	1.4	5325	2890	2676	2677
ZnO	5606	125	3.4	5435	2949	2731	2730
ZrO_2	5600	244	8.0	7596	4122	3817	3781

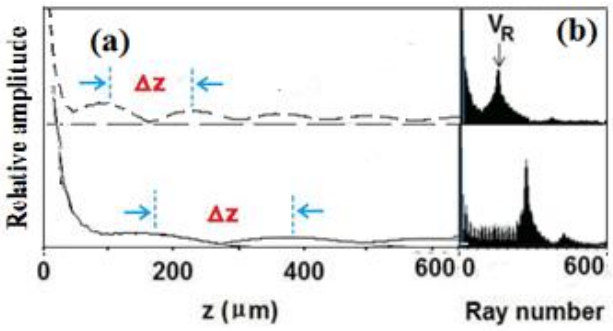

Fig. 1. Acoustic signatures (a) for ceramic substrates: BN (- - -) and Al_2O_3 (——) and (b) their corresponding FFT spectra

The spacing between two successive maxima or successive minima, known as Δz, differs from one material to the other, e.g., it is smaller in BN than in Al_2O_3. This oscillatory behavior is treated via fast Fourier transform, FFT, analysis. The obtained spectra are displayed in Fig. 1b. It is well established that under normal operating conditions of a SAM, the most dominating mode is the

Rayleigh one. Hence, the principal peak obtained in FFT spectra (Fig. 1b) represents such a mode form which the Rayleigh velocity, V_R, is deduced according the following formula [5]:

$$V_R = V_{liq.}/[1 - (V_{liq.}/2f\Delta z)^2]^{1/2} \quad (5)$$

The results, thus obtained, are regrouped in Table 1 (last column) for Rayleigh velocities of all investigated ceramics. These values are close to those obtained via the one parameter approach.

3.2. Dependence of adhesion energy on SAW velocities

The variations of the energy of adhesion on Rayleigh velocity for different nonreactive metals (Au, Cu, Sn, Ga and Ag) deposited on different ceramics are investigated. We consider some published data on energy of adhesion for different metals/ceramics systems [2, 13 - 22]. The obtained results are presented below.

3.2.1. Gold/ceramic substrate systems

To investigate the effects of the energy of adhesion on Rayleigh velocity for different metal/ceramic combinations, we first consider gold/ceramic substrates systems (Al_2O_3, BN, CoO, Er_2O_3, Ho_2O_3, Lu_2O_3, SiC, SiO_2, TiC, TiO_2, Ti_2O_3, Y_2O_3, Yb_2O_3); the obtained results are illustrated in Fig. 2.

It can clearly be seen that the energy of adhesion increases linearly with Rayleigh velocity for all types of substrates. However, we notice the existence of two sets of results gathering around two parallel lines; the continuous lines represent the best fit. In fact, the higher values of the systems Au/CoO, Au/TiC, Au/Ti_2O_3, Au/Yb_2O_3, fall on the upper curve. Whereas, the lower curve concerns other systems with smaller W_{ad} values (Au/BN, Au/Lu_2O_3, Au/SiC, Au/Er_2O_3, Au/SiO_2, Au/TiO_2, Au/Y_2O_3).

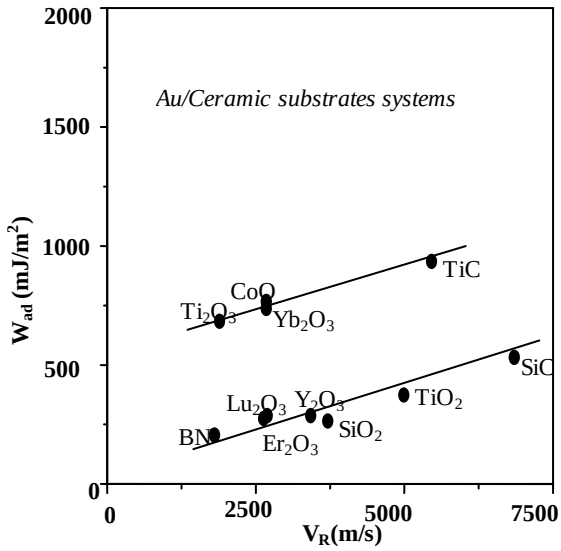

Fig. 2. Energy of adhesion as function of calculated Rayleigh velocities of gold on different ceramic substrates; the lines are the best fit

3.2.2. Different metals/ceramic substrate systems

In order to generalize the above observations obtained with Au/ceramic substrate systems and to put into evidence the results reproducibility, we considere several other metal/ceramic substrates, i.e., the systems:

- Cu/(A1N, Al_2O_3, BN, CoO, NiO, SiO_2, TiO, ZnO, ZrO_2) ceramic substrates,
- Sn/(A1N, BN, CoO, Lu_2O_3, MgO, NiO, SiC, SiO_2, TiO, Yb_2O_3) ceramic substrates
- Ga/(AIN, Al_2O_3, CoO, MgO, NiO, SiO_2, TiO, ZnO, ZrO_2) ceramic substrates
- Ag/(AIN, Al_2O_3, BN, CoO, MgO, NiO, SiO_2, TiO, ZrO_2) ceramic substrates

The obtained results are illustrated in Fig. 3 in terms of energy of adhesion as a function of Rayleigh velocity for several non reactive metals Au (□ □ □), Cu (○○○), Sn (△△△), Ga (▽▽▽), Ag (▷▷▷) on different substrates. All the curves show the same behavior: the energy of adhesion increases linearly with increasing V_R. However, we distinguish two sets of linear dependences that are regrouped according to the band gap energy of the substrate, as discussed below.

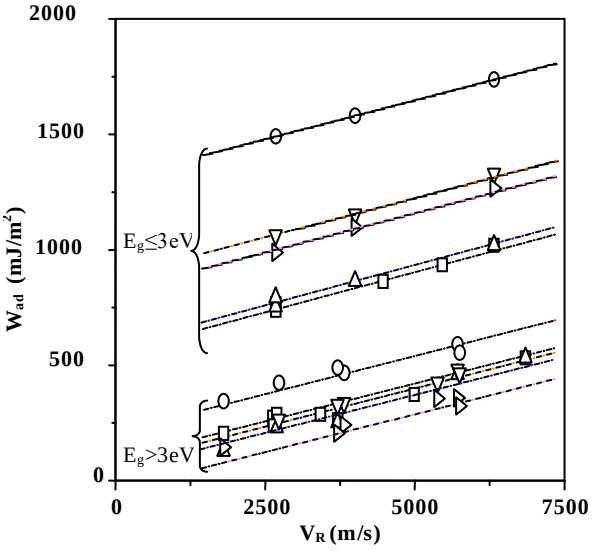

Fig. 3. Energy of adhesion as function of calculated Rayleigh velocities for several metals: Au (□ □ □), Cu (○○○), Sn (△△△), Ga (▽▽▽), Ag (▷▷▷) on different ceramic substrates; the lines are the best fit

3.3. Quantification of the results and discussion

The dependence of W_{ad} on $V_{R(Au)}$ is quantified via curve fitting, (lines in Figs. 2 and 3). We distinguish two parallel dependences for gold-ceramic substrate systems: for higher energy values (upper curve) the linear variation is found to be of the form:

$$W_{ad}] = 0.07V_{R(Au)} + 553 \quad (6a)$$

Whereas, for small energy values (lower curve), the linear dependence is found to be of the form:

$$W_{ad}] = 0.07V_{R(Au)} + 76 \quad (6b)$$

Moreover, it should be noted that the same behavior of two parallel lines is obtained for all metal/ceramic substrate systems. The exact corresponding equation of each material/ceramic system is found to be as follows:

a) For small gap materials:

$$W_{ad}]_{Cu} = 0.07V_{R(Cu)} + 1309 \quad (7a)$$
$$W_{ad}]_{Sn} = 0.07V_{R(Sn)} + 602 \quad (7b)$$
$$W_{ad}]_{Ag} = 0.07V_{R(Ag)} + 991 \quad (7c)$$
$$W_{ad}]_{Ga} = 0{,}07V_{R(Ga)} + 863 \quad (7d)$$

b) For large gap materials:

$$W_{ad}]_{Cu} = 0.07V_{R(Cu)} + 228 \quad (8a)$$
$$W_{ad}]_{Sn} = 0.07V_{R(Sn)} + 37 \quad (8b)$$
$$W_{ad}]_{Ag} = 0.07V_{R(Ag)} + 14 \quad (8c)$$
$$W_{ad}]_{Ga} = 0{,}07V_{R(Ga)} + 78 \quad (8d)$$

Therefore, all curves satisfy the same relation not only for small gap materials but also for large gap ceramics; the general expression takes the form:

$$W_{ad}]_{mat.} = 0.07\ V_{R(mat.)} + C \quad (9)$$

where the subscript, $_{mat.}$, represents any given investigated material (Au, Cu, Sn, Ga, Ag) and C is a characteristic constant for each metal/ceramic combination.

The similar dependence (with the same slope = 0.07) is indicative of the existence of the same mechanism responsible for this behavior. However the existence of two parallel dependences for every system is due to the energy band structure of the ceramic materials in particular the energy gap (Table 1). A close analysis of Fig. 3 and the E_g column clearly shows that the upper set of curves corresponds to solid materials with small energy gaps ($E_g \leq 3$ eV), whereas the lower ensemble of curves represents materials with large energy gaps ($E_g > 3$ eV).

In fact, solid materials with small band gaps behave as conductors ($E_g \rightarrow 0$) or semiconductors (Eg ≤ 3 eV). In this case, it was reported [23] that the high energy values of the non-reactive metal-ceramic solid systems are associated with high electron density of metals and low band gap energy of solids, and vice versa. The adhesion between a metal and a ceramic crystal is assured by the electron transfer and is enhanced as the intensity of the electron transfer at the metal/ceramic interface is increased. For large bandgaps, there will be practically no free charges inside the ceramic crystal. In this case, the electron transfer at metal/ceramic interfaces cannot be taking place [2].

Hence, the discrepancy in C values for a given metal/small gap ceramics and the same metal/large gap ceramics could be explained by the fact that for $E_g > 3$ eV, there will be a small density of free carriers and consequently less electron transfer. Thus leading to smaller C values for large gap ceramics.

The importance of the deuced relation (9) lies in its applicability to all investigated metal/ceramic systems. It could be extended, through familiar relations, to other elastic parameters. Similar results for longitudinal and transverse velocities were obtained. Moreover, preliminary results for elastic constants (Young's modulus and shear modulus) are very satisfying.

4. Conclusions

In this work, the adhesion energy as a function of surface acoustic wave velocities are investigated for several metals (Au, Cu, Sn, Ga and AG) on a great number of ceramic substrates (AlN, Al_2O_3, Bn, CoO, Er_2O_3, Ho_2O_3, LaB_6, Lu_2O_3, MgO, NiO, SiC, SiO_2, Si_3N_4, TiC, TiO, TiO_2, Ti_2O_3, Y_2O_3, Yb_2O_3, ZnO And Zr_2O_3). Elastic parameters (acoustic signatures, surface acoustic wave velocities velocities) were determined for all cases. It was shown that the energy of adhesion increases linearly with Rayleigh velocity for all types of substrates. This universal relation that could be extended to other acoustic parameters is applicable to all metal/ceramic combinations.

References

[1] F. E. Kennedy in: "Encyclopedia of Physics", eds, Lerner and Trigg, Wiley-VCH, Weinheim, 2005.
[2] J. G Li, Mat. Lett. **22,** 169 (1995).
[3] L. Viktorov, "Rayleigh and Lamb Waves", Plenum Press, New York, 1967.
[4] M. Doghmane, F. Hadjoub, A. Doghmane and Z. Hadjoub, Mater. Lett. **61,** 813 (2007).
[5] J. Kushibiki, N. Chubachi, IEEE Trans. Sonics and Ultrasonics, SU-32, 189 (1985).
[6] R. G. Maev, "Acoustic Microscopy: Fundamentals and Applications", Wiley-VCH, Berlin, 2008.
[7] G A. D. Briggs, O. V. Kolosov "Acoustic Microscopy", Oxford Univ. Press, Oxford, (2010).
[8] C. G R. Sheppard, T. Wilson, Appl. Phys. Lett. **38**, 858 (1981).
[9] A. Doghmane, S. Douafer, Z. Hadjoub, J. Optoelectron. Adv. M. **16**(11-12), 1339 (2014).
[10] P. V. Zinin, in Handbook of Elastic Properties of Solids, Liquids and Gases, eds. Levy, Bass and Stern, Academic Press, New York, 2001.
[11] A. Briggs, "Advances in Acoustic Microscopy", vol. **1**, Plenum Press, New York, 1995.
[12] W. H. Strehlow, E. L. Cook, J. Phys. Chem. Ref. Data **2**, 163 (1973).
[13] Yu. V. Naidich, Prog. Surf. Membr. Sci. **14**, 353 (1981).
[14] M. N. Tikkanen, S. Ylaisaari, K. Blomster, Phys. Sintering **3**, 1 (1971).
[15] Yu. V. Naidich, V. S. Zhuravlev, N. I. Frumina, J. Mater. Sci. **25**, 1895 (1990).

[16] J. G. Li, Scripta Metall. Mater. **30,** 337 (1994).
[17] N. Y. Taranets, Y. V. Naidich, Powder Metall. Met. Ceram. **35,** 74 (1996).
[18] H. Goretzki, W. Scheuermann, High Temp. High Pressures **3**, 649 (1971).
[19] F. L. Harding, D. R. Rossington, J. Am. Ceram. Soc. **53**, 87 (1970).
[20] Yu. V. Naidich, V. S. Zhuravlev, N. I. Frumina, V. V. Leshneva, P. A. Verkhovodov, Porosh. Metall. **6**, 73 (1985).
[21] J. G. Li, Rare Metals **12**, 84 (1993).
[22] J. G. Li, H. Hausner, Mater. Lett. **11**, 355 (1991).
[23] J. G. Li, J. Mater. Sci. Lett. **11**, 903 (1992).

*Corresponding author: a_doghmane@yahoo.fr